The Arg7Lys Mutant of Heat-Labile Enterotoxin Exhibits Great Flexibility of Active Site Loop 47−56 of the A Subunit[†,||]

Focco van den Akker,[‡] Ethan A. Merritt,[‡] MariaGrazia Pizza,[§] Mario Domenighini,[§] Rino Rappuoli,[§] and Wim G. J. Hol*[,‡]

Departments of Biological Structure and Biochemistry, Biomolecular Structure Center and Howard Hughes Medical Research Institute, University of Washington, SL-15, Seattle, Washington 98195, and Immunobiological Research Institute Siena (IRIS), Via Fiorentina 1, 53100 Siena, Italy

Received March 23, 1995; Revised Manuscript Received June 9, 1995[⊗]

ABSTRACT: The heat-labile enterotoxin from *Escherichia coli* (LT) is a member of the cholera toxin family. These and other members of the larger class of AB_5 bacterial toxins act through catalyzing the ADP-ribosylation of various intracellular targets including $G_{s\alpha}$. The A subunit is responsible for this covalent modification, while the B pentamer is involved in receptor recognition. We report here the crystal structure of an inactive single-site mutant of LT in which arginine 7 of the A subunit has been replaced by a lysine residue. The final model contains 103 residues for each of the five B subunits, 175 residues for the A_1 subunit, and 41 residues for the A_2 subunit. In this Arg7Lys structure the active site cleft within the A subunit is wider by approximately 1 Å than is seen in the wild-type LT. Furthermore, a loop near the active site consisting of residues 47−56 is disordered in the Arg7Lys structure, even though the new lysine residue at position 7 assumes a position which virtually coincides with that of Arg7 in the wild-type structure. The displacement of residues 47−56 as seen in the mutant structure is proposed to be necessary for allowing NAD access to the active site of the wild-type LT. On the basis of the differences observed between the wild-type and Arg7Lys structures, we propose a model for a coordinated sequence of conformational changes required for full activation of LT upon reduction of disulfide bridge 187−199 and cleavage of the peptide loop between the two cysteines in the A subunit. These proposed conformational changes start at the site of reduction and cleavage and propagate a distance of over 20 Å to affect the active site itself.

Heat-labile enterotoxin (LT)[1] is a hexameric protein secreted by enterotoxigenic strains of *Escherichia coli* and is highly homologous to cholera toxin (CT) secreted by *Vibrio cholerae*. Both proteins are major virulence factors. LT acts similarly to CT, causing acute infectious diarrhea. This can lead to effects varying from a mild "traveller's diarrhea" to dehydration and death, especially among young children in developing countries (Black, 1986). The two proteins belong to a larger class of bacterial toxins which share a similar A/B functional arrangement (Gill, 1976). The B chain is responsible for receptor recognition and delivers the catalytic part of the toxin, the A subunit, to the target cell. In LT and CT the B subunits form a pentamer which specifically recognizes G_{M1} gangliosides on the membrane of the target intestinal epithelial cells. G_{M1} binding by the B pentamer is the first step of LT and CT action (Van Heyningen, 1983; Eidels et al., 1983), which is then followed by membrane translocation of the A subunit into the cell interior. Full activity requires the A subunit to be "nicked" proteolytically between residues 192 and 195, splitting it into an N-terminal A_1 fragment and a smaller A_2 fragment (Moss et al., 1981). After nicking, A_1 and A_2 are still linked by a disulfide bond between residues 187 and 199. For full activation this disulfide must be reduced to yield the free A_1 subunit containing the catalytic ADP-ribosylating activity (Mekalanos et al., 1979a; Tomasi et al., 1979). Once in the cell, the A_1 fragment ADP-ribosylates Arg201 of the α-subunit of the stimulatory protein G_s of the adenylate cyclase system (Cassel & Pfeuffer, 1978).

The catalytic mechanism of LT and CT is not yet known in structural detail, but mutagenesis studies and superposition of homologous residues in related ADP-ribosylating toxins have pointed out residues important for activity. In the active site of diphtheria toxin (DT), exotoxin A (ETA), pertussis toxin (PT), cholera toxin (CT), and heat-labile enterotoxin (LT), a single glutamic acid is conserved (Allured et al., 1986; Choe et al., 1992; Sixma et al., 1991; Stein et al., 1994). In heat-labile enterotoxin this is Glu112, which has been shown by mutagenesis studies to be important for ADP-ribosyltransferase activity (Tsuji et al., 1990, 1991). Photolabeling studies in ETA and DT (Carrol & Collier, 1984, 1987) further suggest that this glutamic acid side chain is located near the NAD binding pocket. Mutagenesis studies, kinetic measurements, and ligand binding studies on ETA, DT, and PT have shown that the replacement of the

[†] This research was supported by the NIH (AI34501) and by an equipment grant from the Murdock Charitable Trust.

[||] The coordinates of the A:Arg7Lys mutant of LT have been deposited in the Brookhaven Protein Data Bank (file name 1LTG).

* Author to whom correspondence should be addressed at the Department of Biological Structure [Fax: (206) 543-1524].

[‡] University of Washington.

[§] Immunobiological Research Institute Siena (IRIS).

[⊗] Abstract published in *Advance ACS Abstracts,* August 1, 1995.

[1] Abbreviations: CT, cholera toxin; DT, diphtheria toxin; ETA, exotoxin A; LT, *Escherichia coli* heat-labile enterotoxin type I; PT, pertussis toxin; ApUp, adenylyl-3′,5′-uridine monophosphate; ADP, adenosine 5′-diphosphate, G_{M1}, Gal(β1−3)GalNAc(β1−4){NeuAc(α2−3)}Gal(β1−4)Glc(β1−1)-ceramide; G_s, stimulatory G protein; $G_{s\alpha}$, α-subunit of the stimulatory G protein; NAD, β-nicotinamide adenine dinucleotide; rms, root mean square.

0006-2960/95/0434-10996$09.00/0

conserved Glu greatly reduces ADP-ribosyltransferase activity while causing only minimal changes in affinity for NAD (Douglas & Collier, 1990; Wilson et al., 1990; Antoine et al., 1993). The conserved Glu is thus likely to be intimately involved in catalyzing the transfer of an ADP-ribose moiety from NAD to $G_{s\alpha}$. Glu110 in LT, although not totally conserved in the other ADP-ribosylating toxins, has also been pointed out to be critical for toxic activity (Lobet et al., 1991). Ser61 is also not conserved, but when this residue is substituted by a Phe, a dramatic decrease in activity in LT is observed (Harford et al., 1989).

Mutation studies of LT and CT have also implicated Arg7 as an important residue. When Arg7 is mutated into a lysine, the ADP-ribosylating activity is decreased dramatically in both CT and LT (Lobet et al., 1991; Burnette et al., 1991; Pizza et al., 1994). This residue is also conserved in pertussis toxin (PT), and it has been suggested by photolabeling studies that mutation of this side chain in PT most likely affects NAD binding (Cieplak et al., 1990). In the latent (unnicked, unreduced) LT structure (Sixma et al., 1991, 1993), as well in the partially activated (nicked, unreduced) LT structure (Merritt et al., 1994a), Arg7 is located at the bottom of the active site crevice. The Arg 7 side chain is virtually inaccessible to solvent as the guanidinium group is involved in an extensive hydrogen-bonding network. The present paper reports crystallographic studies carried out on the Arg7Lys mutant of the A_1 subunit of LT in order to investigate its critical role for the toxic activity.

EXPERIMENTAL PROCEDURES

The A_1:Arg7Lys mutant, hereafter called the "Arg7Lys" mutant, of heat-labile enterotoxin (LT) from *E. coli* was overexpressed and purified as described by Pizza et al. (1994). The mutant toxin was crystallized in a manner similar to that of the wild-type toxin using a modified version of the capillary method previously reported (Pronk et al., 1985). The binding modes of the substrates NAD and $G_{s\alpha}$ to LT are still unknown at present. For this reason an attempt was made to crystallize the inactive-latent LT Arg7Lys mutant in the presence of 18 mM NAD and 0.8 mM guanyltyramine with the hope of obtaining crystals of a protein−substrate complex. Concentrations for both the substrates are well above the measured binding constants for these two substrates [4 mM for NAD (Moss et al., 1976) and 44 μM for guanyltyramine (Mekalanos et al., 1979b)].

The mutant protein (10 mg/mL) was equilibrated by dialysis against 400 mM NaCl and TEA (100 mM Tris-HCl, pH 7.5, 1 mM EDTA, and 0.02% sodium azide). The following layers were added to the capillary: 5 μL of the buffered protein solution, 5 μL of 42.5 mM NAD, 2 mM guanyltyramine in 100 mM NaCl in TEA buffer, and 2 μL of 40% PEG 6000 in TEA buffer. The final concentrations in the crystallization capillary are 4.2 mg/ml LT mutant, 18 mM NAD, 0.8 mM guanyltyramine, 210 mM NaCl, and 6.7% PEG. Crystals grew in several weeks at room temperature in space group $P2_12_12_1$ with cell dimensions $a = 119.7$ Å, $b = 98.5$ Å, and $c = 65.5$ Å. This means that the Arg7Lys crystal is virtually isomorphous with native LT, which crystallizes in the same space group with cell dimensions $a = 119.2$ Å, $b = 98.2$ Å, and $c = 64.8$ Å (Pronk et al., 1985). As the Arg7Lys mutant has been shown to be more susceptible to proteolysis (Lobet et al., 1991), both the starting protein solution and dissolved crystals were examined on a SDS−PAGE gel, which indicated that the A subunit is still intact (data not shown). For data collection a single crystal was used with a size of 1.0 × 0.2 × 0.2 mm. Diffraction images corresponding to 0.2° oscillation of the crystal were collected at room temperature using a Siemens X100 multiwire area detector mounted on a Rigaku RU200 anode. The program XENGEN (Howard et al., 1987) was used for integration and data processing. The crystal diffracted to 2.4 Å resolution, with an overall merging R-factor on intensities of 7.3% (Table 1).

Table 1: Data Collection Statistics of the Arg7Lys Mutant of Heat-Labile Enterotoxin

space group	$P2_12_12_1$
cell dimensions	119.7, 98.5, 65.5 Å
diffraction limit	2.4 Å
no. of total measurements	60 917
no. of unique reflections (10−2.4 Å)	22 826 ($F > 2\sigma_F$)
R_{merge} (on I)	7.3%
completeness	75%
completeness in shell 2.40−2.48 Å	54%

The structure of the Arg7Lys mutant of LT was solved starting from the 1.95 Å native structure (Sixma et al., 1993). A rigid body refinement (using data from 10.0 to 2.8 Å), treating the five B subunits (each 103 residues) and the A_1 (residues 4−188) and the A_2 fragments (residues 196−236) as separate chains, brought the crystallographic R-factor down from 0.292 to 0.255 using X-PLOR (Brunger et al., 1987). This was followed by refining individual atomic position and B-factors with arginine 7 deleted from the protein model. In the subsequently calculated omit map lysine 7 could be built in well-defined $F_o - F_c$ electron density. The program O was used for model building (Jones et al., 1991). The initial refinement steps were followed by positional and individual B-factor refinement for all protein atoms. The crystallographic R-factor at this stage was 0.183 using data from 10.0 to 2.8 Å. Density corresponding to residues 47−56 of the A_1 subunit could not be located in either $2F_o - F_c$ or $F_o - F_c$ maps in which these residues were omitted from the model. As a molecular dynamics annealing refinement protocol had been successful in obtaining the correct conformation of a loop when starting from a significantly different conformation (Wierenga et al., 1991), a similar approach was used for the Arg7Lys structure at this stage by using a slow-cooling procedure in X-PLOR (Brunger et al., 1990). The temperature during the slow-cooling protocol was gradually brought down from 3000 to 300 K. This was followed again by positional and individual B-factor refinement. As residues 47−56 did not move into density as a result of the molecular dynamics simulation, and the loop containing residues 47−56 still could not be located elsewhere in omit $F_o - F_c$ maps, these residues were omitted from the model in the following rounds of refinement. During subsequent steps in refinement a few ϕ,ψ angles and side chains were manually adjusted to fit into the electron density. Also 71 solvent molecules were added to the model, and the resolution of data used for refinement was extended to 2.4 Å. The solvent molecules added were observed as peaks greater than 3σ in σ_A-weighted (Read, 1986) $F_o - F_c$ electron density maps and had reasonable hydrogen-bonding geometry. The final R-factor after refinement using data between 10.0 and 2.4 Å was 17.8%.

Table 2: Refinement Statistics of the Structure of the Arg7Lys Mutant of Heat-Labile Enterotoxin

resolution range	10−2.4 Å
no. of reflections	22 826 ($F > 2\sigma_F$)
residues in model	731
solvent molecules	71
R-factor	17.8%
rms deviation from ideality	
bond distance	0.013 Å
bond angles	2.96°
dihedrals	24.0°
improper dihedrals	1.99°

RESULTS

Quality of the Molecular Model. The final model of the Arg7Lys mutant of heat-labile enterotoxin consists of 731 residues and 71 solvent molecules. A total of 24 residues are not well defined in electron density maps and have been omitted from the model. These residues are all in the A subunit and include N-terminal residues 1−3, C-terminal residues 237−240, and residues 189−195, all of which were also ill-defined in the wild-type 1.95 Å structure (Sixma et al., 1993). Additionally, residues 47−56 from the A subunit in the Arg7Lys mutant also could not be located (Figure 2a,b) and thus are not included in the model. The final model yields a crystallographic *R*-factor of 17.8% for 22826 unique reflections to 2.4 Å resolution with good stereochemistry (Table 2).

Overall Structure. The overall structure of Arg7Lys LT is very similar to that of the wild-type toxin. The B pentamer is 25 Å distant from the site of the introduced mutation and is essentially unaffected by the mutation. Superposition of the B pentamer of the mutant onto the wild-type toxin yields an rms deviation of 0.27 Å for the 515 Cα atoms in the five chains of 103 residues. The largest deviations in the B pentamer occur in the loop 50−60, which has been previously observed to be of variable conformation in the absence of bound receptor or receptor fragments (Sixma et al., 1993; Merritt et al., 1994b).

When the B pentamer of the wild-type and mutant toxins are superimposed, the corresponding A subunits deviate by only 0.57 Å for all Cα atoms. When the A subunits are superimposed directly, the rms deviation for these Cα atoms of the A subunit is 0.53 Å (see Figure 1a). Although it has been observed that there can be considerable variation in the orientation of the A subunit with respect to the B pentamer (Sixma et al., 1992), in this case the angular relationship of the A subunit with respect to the B pentamer is virtually the same (0.8° difference) in the wild-type and mutant structures. Also, the overall mobilities are virtually the same: the average *B*-factor of the wild-type A_1 subunit is 38 Å^2, and that of the mutant is also 38 Å^2. The *B*-factors for main-chain atoms per residue as plotted in Figure 1b are also very similar to those observed in the A subunit of the wild-type toxin with the exception of a few loops indicated

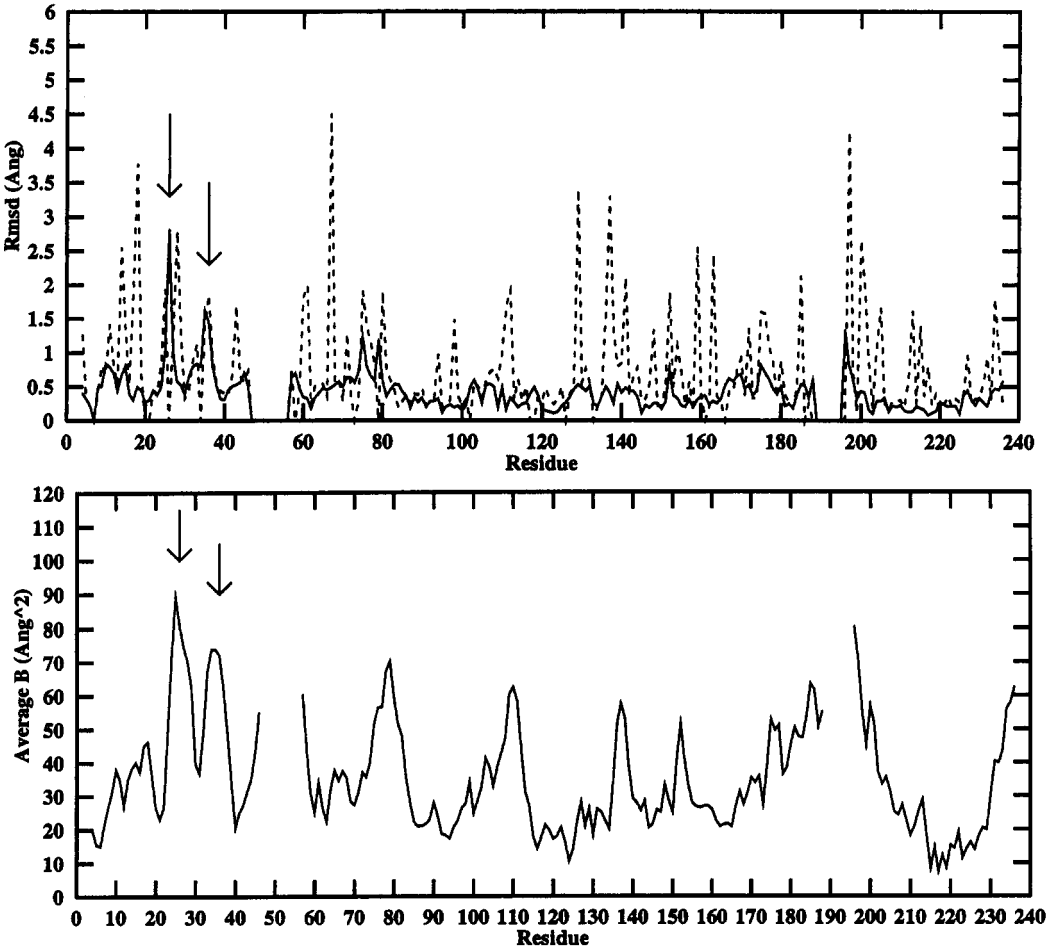

FIGURE 1: (a, top) rms differences in main-chain (in solid line) and side-chain (in dashed line) coordinates for the catalytic A subunit when the structure of the Arg7Lys mutant and the native 1.95 Å structure of LT are compared (Sixma et al., 1993). The arrows highlight loop residues 25−27 and 33−36 which have the largest main-chain atom shifts. No shift is given for residues 47−56 since these are invisible in the Arg7Lys structure of LT. (b. bottom) Plot of the averaged main-chain *B*-factors per residue in the A subunit of the Arg7Lys mutant of LT. The two arrows indicate two other regions with an increase in thermal motion, besides loop 47−56, compared to the wild-type LT.

Table 3: Hydrogen Bonds of Residue 7

(a) Hydrogen Bond Interactions of Side-Chain A:Arg7 in the Wild-Type LT Structure	
Arg7 hydrogen bonds in wild-type LT	distance (Å)
NE (Arg7)−OD2 (Asp9)	2.7
NH1(Arg7)−O (Arg54)	3.2
NH1(Arg7)−O (Ser61)	3.1
NH2(Arg7)−OD2 (Asp9)	2.9
NH2(Arg7)−O (Val53)	3.0
(b) Nearest Neighboring Atoms of Side-Chain A:Lys7 in the Arg7Lys Mutant of LT	
Lys7 interactions in Arg7Lys LT	distance (Å)
NZ (Lys7)−O (Ser61)	4.4
NZ (Lys7)−O (Ala8)	3.5
NZ (Lys7)−OD2 (Asp9)	3.6

by arrows. Unfortunately, but not unexpectedly in view of the lack of activity of the Arg7Lys mutant, no electron density could be observed for either NAD or guanyltyramine. Even though the overall structures of the A subunits of wild-type and Arg7Lys mutant toxins are very similar, there are nevertheless distinct differences as will be discussed below.

Lys7 in the Arg7Lys Mutant. In the wild-type toxin, Arg7 is engaged in not less than five quite strong hydrogen bonds (see Table 3a and Figure 2c). By means of these interactions the guanidinium group links two β strands together at the bottom of the active site cleft [see also Figure 19a in Sixma et al. (1993)]. The guanidinium group is not only engaged in a very intricate network of hydrogen bonds to a number of residues which have been shown to be very important for catalysis but also interacts via two hydrogen bonds with residues in loop 47−56 (Figure 2b). This is of great potential importance as we will discuss below.

The electron density for Lys7 in the Arg7Lys mutant of LT is well-defined (Figure 2a), as reflected by an average *B*-factor of 22 Å^2 for the lysine side-chain atoms. The average *B*-factor for the Arg7 side chain in wild-type toxin is also 22 Å^2. Hence the mutation has not caused any dramatic change in mobility of Lys7 compared to Arg7 in wild-type toxin.

Although the substitution of Arg by Lys is usually considered to be conservative, the interactions which Lys7 makes with its environment in the Arg7Lys mutant are dramatically different from those of Arg7 in the wild-type toxin. The number of interactions made by the lysine side chain is virtually zero although a few very long hydrogen bonds may be considered to exist (Table 3b, Figure 2d). This difference in number of interactions is not due to a significant change in the position or orientation of the residue 7 side chain itself. The Cα, Cβ, and Cγ atoms of Arg7 and Lys7 differ by only 0.38, 0.23, and 0.65 Å, respectively. However, the shorter length of the lysine side chain together with an unexpected conformational change of loop 47−56 which previously interacted with the guanidinium group of Arg7 reduces the number of interactions dramatically. The solvent accessibility of the Lys7 side chain is 40.6 Å^2, calculated using the program MSCON (Connelly, 1983). The corresponding solvent accessibility for the Arg7 side chain in the wild-type toxin is 3.3 Å^2. This clearly shows that the side chain of Lys7 has become much more solvent accessible.

Environment of Lys7 in the Arg7Lys Mutant. A major difference between wild-type and mutant toxin is the state of the loop comprising residues A:47−56 (Figure 2a,b). We conclude that as a result of the Arg7Lys mutation the loop comprising residues A:47−56 has become too mobile to give a clear signal in our 2.4 Å resolution electron density maps.

The displacement of loop 47−56 is associated with smaller conformational shifts in other nearby loops in the A subunit (Figure 1a and 3), specifically the loop comprising residues 25−27 and loop 33−36. These shifts are accompanied by an increase in disorder of both loops when compared to the wild-type toxin (Figure 1b). It is noteworthy that residues of loop A:25−27 are in contact with loop A:47−56 through a hydrogen bond of the backbone carbonyl oxygen of Tyr55 with the backbone nitrogen of Arg25. Residues of loop A:25−27 interact also with residues in loop A:33−36. The possible importance of these interactions will be pointed out in the discussion below.

A third difference in the active site is more subtle and concerns the width of the active site cleft of which Arg7 forms the "floor". Substitution of the Arg residue by a Lys not only allows the active site to become more accessible as loop residues A:47−56 move away but also allows the active site crevice to widen by about 1.0 Å. This is illustrated by the fact that the distance between the Cα atoms of residues pairs Asp9−His44 and Ile76−His107 increases by approximately 1.0 Å (see Figure 4).

DISCUSSION

Why Is the Arg7Lys Mutant Inactive? The Arg7Lys structure presented in this paper shows a remarkable displacement of loop 47−56 located near the active site. The local disorder of loop residues 47−56 observed in the A subunit is also consistent with the increased sensitivity to trypsin of the Arg7Lys mutant (Lobet et al., 1991) compared to the wild-type A subunit.

There are several possible reasons why the Arg7Lys mutant of LT might be inactive, which we will discuss in turn.

(i) The arginine side chain may perform a crucial function in substrate binding. There is considerable evidence suggesting that Arg7 performs an important role in binding the substrate NAD. In PT, the homologue of the Arg7 side chain, which is Arg9, has been implicated in NAD binding (Cieplak et al., 1990). Also in DT there are several consistent lines of evidence that the homologue of the Arg7 side chain, which is His21, is involved in an interaction with NAD:

(a) The structure of diphtheria toxin complexed with the inhibitor ApUp shows a hydrogen bond between the adenosine ribose moiety of the inhibitor and His21 of the toxin (Bennett et al., 1994). Since ApUp and NAD share an adenosine group, and the active sites of LT and DT show structural similarities (Sixma et al., 1991), Choe et al. (1992) postulate that the adenosine moiety of NAD binds to this family of ADP-ribosylating toxins in a similar way. In order to accommodate such a binding mode in LT and CT, the residues comprising loop 47−56 will have to move away from the position they are seen to occupy in the wild-type LT/CT structure (see Figure 5). (This conclusion is derived by superimposing the active sites of DT and LT as is further discussed below.) This move of loop 47−56 is perfectly possible as evidenced by our Arg7Lys structure described in this paper.

(b) Fluorometric assays of NAD binding and diethyl pyrocarbonate modification of DT show that His21 in DT is involved in NAD binding (Papini et al., 1989, 1990). On

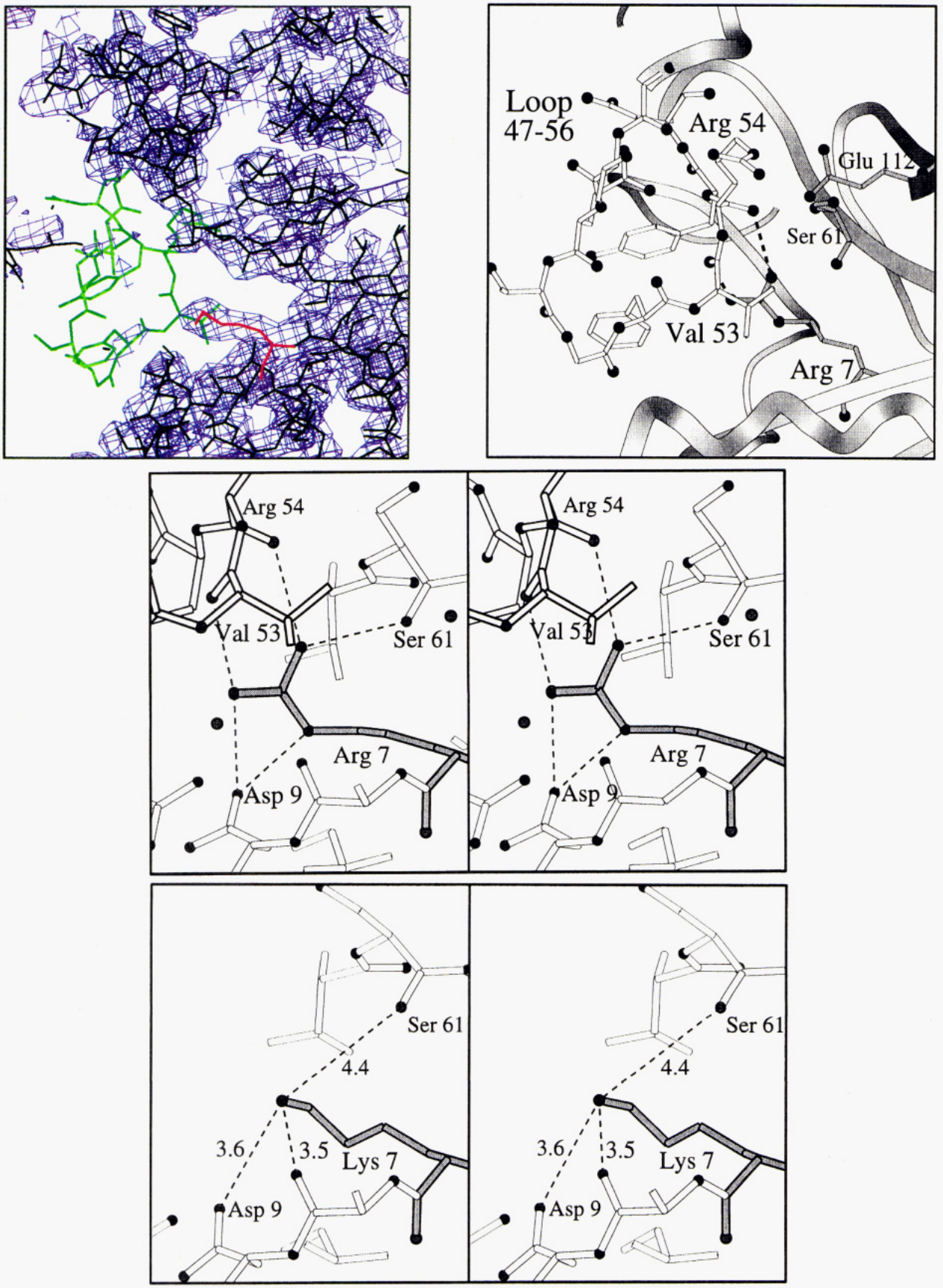

FIGURE 2: (a, top left) $2F_o - F_c$ electron density of the active site of the Arg7Lys mutant of LT contoured at the 1.0σ level. Lysine 7 is shown in red. The native position of loop 47−56 is shown in green, and no density for these residues could be located in the mutant structure. (b, top right) Close-up view of the active site of the wild-type LT. Residues 7, 61, 112, and 47−56 shown in ball-and-stick representation illustrating the two hydrogen bonds of the Arg7 side chain with loop 47−56 via the main-chain atoms of Val53 and Arg54. This figure was generated using the program MOLSCRIPT (Kraulis, 1991). (c, middle) Close-up stereoview of all five hydrogen bonds the Arg7 side chain makes in the wild-type LT structure. (d, bottom) Close-up view of Lys7 and neighboring residues in the A subunit of the Arg7Lys mutant of LT. Interatomic distances between selected atoms are given in angstroms. As summarized in Table 3b, the lysine residue is not engaged in any hydrogen bonds.

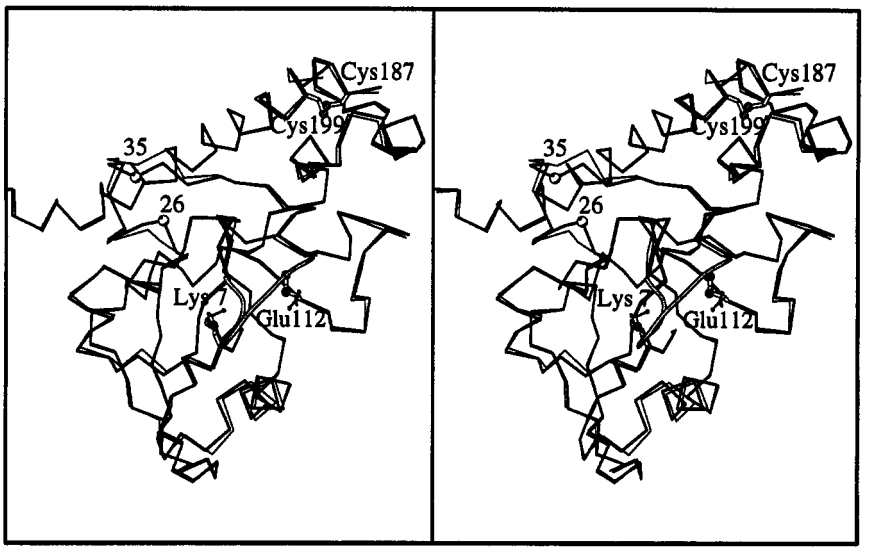

FIGURE 3: Superposition of the A subunits of wild-type LT (in thin lines) and the Arg7Lys mutant of LT (in thick lines). The proteolysis loop linking A_1 and A_2 comprising residues 189−195 is mobile and not depicted. Loop 47−56 is flexible in the Arg7Lys mutant and is only depicted for the wild-type protein in coil representation. The Cα atoms of residues 26 and 35 are shown to highlight the regions where significant changes occur in the Arg7Lys mutant structure compared to the wild-type LT structure. Shown in ball-and-stick representation are residues Arg7, Glu112, Cys187, and Cys199.

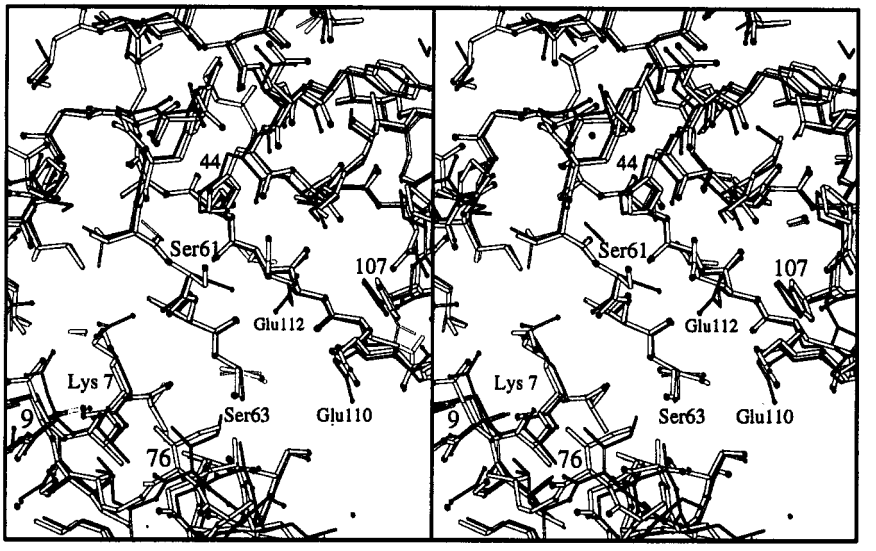

FIGURE 4: Superposition of the A subunits of wild-type LT shown in thin lines and the A subunit of the Arg7Lys mutant in thick lines. Highlighted are the following active site residues: Arg7/Lys7, Ser61, Ser63, Glu112 and Glu110.

the basis of the observation that both NAD and adenosine are effective in protecting His21 from modification while adenine is not, Papini et al. (1989) postulated that His21 is in very close proximity to the binding site of the ribose moiety of adenosine in NAD. This is in perfect agreement with the adenosine binding mode obtained from the ApUp−DT complex as mentioned above.

(c) Mutations of this same residue, DT His21, have been shown to affect the binding constant of NAD, suggesting that His21 is directly involved in NAD binding (Johnson & Nicholls, 1994).

(ii) The position of loop 47−56 observed in the wild-type enzyme may be crucial for substrate binding. For the reasons just given, it seems most likely that a conformational shift of residues 47−56 away from that seen in the original LT structures is required for substrate binding and catalysis. However, further structural studies will be required to establish the conformation of the 47−56 loop, and of the active site crevice as a whole, during NAD binding and catalysis.

(iii) Replacement of Arg7 by Lys causes the active site crevice to widen by 1.0 Å. Residue Arg7 is located at the bottom of the cleft connecting strand β1 and β3 via a hydrogen bond with the backbone carbonyl of Ser61 (Sixma et al., 1993). Loss of this interaction between the two β strands located at the bottom of the active site crevice might well cause the active site to widen by 1.0 Å, and in an as yet unknown manner (possibly less tight substrate binding) this might result in an inactive toxin.

(iv) Catalysis may require an active site reorganization prevented by the Arg7Lys substitution. The necessary occurrence of an active site conformational change is suggested by the observation that "nicking" and reduction of the A subunit is required for full activity (Moss et al., 1981). Several possibilities concerning conformational changes upon activation and NAD binding will be discussed below. The inability of the Arg7Lys mutant to adopt the conformational changes required for catalysis cannot be ruled out, and additional structural studies of the activated A_1 subunit of LT complexed with one of the substrates are

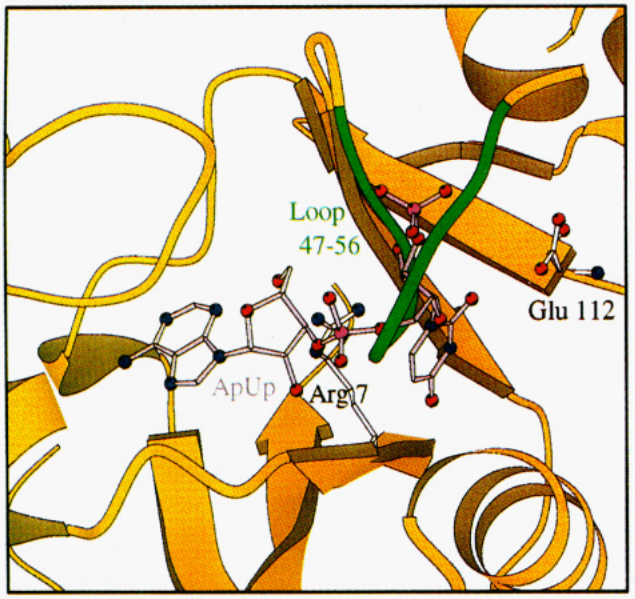

FIGURE 5: Diagram of the superposition of the active sites of native LT and of diphtheria toxin (DT) complexed with ApUp. ApUp is a nanomolar inhibitor of DT which binds competitively with NAD and contains also an adenine nucleotide, and it is thus postulated to be bound in a similar position as in NAD (Choe et al., 1992). DT protein atoms are not shown for clarity (superposition of 38 Cα atoms of DT onto LT resulted in a rms deviation of 1.57 Å between the two structures even though the proteins show very little sequence identity). ApUp is shown in purple, Arg7 and Glu112 of LT are in white, loop 47−56 is in green, and the rest of LT is in yellow. The superposition demonstrates a major clash between the presumed NAD binding position and loop 47−56, indicating that the loop has to move upon NAD binding. The Cα atoms used for the DT/ApUp onto LT superposition are as follows: LT (93−97112−116), 59−73, 4−9, and 83−89; DT (134−138148−152), 52−66, 18−23, and 28−34. If the adenine binding region in DT comprising the small helix residues 28−34 and LT 13−19 is included in the superposition, the rms deviation for all 45 Cα atoms becomes 2.27 Å.

needed to give full insight into the importance of the Arg7 side chain in LT.

We conclude that the Arg7 side chain is most likely involved in an interaction with the substrate NAD and in maintaining structural stability of the active site crevice by means of its hydrogen bond with the backbone carbonyl atom of Ser61.

NAD Binding to LT. There is evidence which suggests that, upon activation of the toxin by nicking and reduction, the 47−56 loop is not immediately displaced or disordered as observed in the Arg7Lys mutant. Proteolysis experiments have shown (Lobet et al., 1991) that the activated A subunit of wild-type LT is more stable than the activated A subunit of the Arg7Lys mutant. This suggests that loop 47−56 in the wild-type A subunit adopts an ordered conformation even after activation and hence is not sensitive to proteolysis. Concerning possible disorder of the loop after NAD is bound, it has been shown that NAD binding to the A_1 subunit of CT decreases the proteolytic sensitivity and thus the overall flexibility (Galloway & van Heyningen, 1987) compared to the unliganded A_1 subunit. This indicates that several flexible parts become more ordered and less susceptible to proteolysis in the A_1 subunit after NAD binding.

The location of a crystallographically determined adenosine binding site observed in exotoxin A (Brandhuber et al., 1988) seems to be in contradiction to the adenosine binding site inferred from the DT−ApUp crystal structure since the two corresponding models for adenosine binding differ by about 10 Å in the location of the adenine ring. In the 2.7 Å structure of the ETA−adenosine complex, the adenine ring is located between residues Tyr470 and Tyr481 (Brandhuber et al., 1988), equivalent to LT residues Ser61 and Ala72, respectively (Sixma et al., 1991). This different position of the adenosine moiety brings the adenosine glycosyl bond close to the catalytically important Glu553, which is equivalent to Glu112 in LT and CT. However, photolabeling studies in both ETA and DT have shown that it is the nicotinamide group of NAD, and not the adenosine moiety, that is in close proximity to the conserved glutamic acid residue (Carroll & Collier, 1984, 1987). Fortunately, the two contradictory binding positions of adenosine can be reconciled. Papini et al. (1991) have found (using photoactivatable derivatives of adenine and adenosine) that the competitive inhibitors adenine, adenosine, and nicotinamide bind in the same region of the active site of DT. Thus Domenighini et al. (1991) suggested that the binding position of adenine observed in ETA is most likely the nicotinamide binding site of NAD. Both moieties, despite their differences, have a conjugated ring system and might thus bind in the same groove, in each case stacking onto Tyr481. So it is the ETA−adenosine structure that most likely reveals where the nicotinamide moiety of NAD binds, and it is the DT−ApUp structure that probably reveals where the adenosine moiety binds to LT and CT.

Activation Mechanism of LT and CT. The mechanism of activation of LT and CT remains an intriguing puzzle since the sites of nicking and reduction are over 20 Å removed from the critical residues Glu112 and Arg7. Full activation of LT and CT requires proteolytic nicking of the 192−195 loop in the A chain as well as reduction of disulfide bridge 187−199 which links the A_1 and A_2 chains (Moss et al., 1981; Mekalanos et al., 1979a; Tomasi et al., 1979). After nicking and reduction, the two fragments A_1 and A_2 are no longer covalently connected. The major noncovalent interactions occur between the long α helix of the A_2 fragment and several loops on the "side" of the triangular A_1 fragment (Sixma et al., 1993). An intriguing question is the pathway by which the active site of the A subunit "senses" the reduction and the nicking of the polypeptide chain. We propose a mechanism for the activation pathway of LT and CT based on the observation that the Arg7Lys structure, even though it corresponds to an inactive form of the toxin, demonstrates the flexibility of the 47−56 loop and exhibits a small but most likely relevant cascade of loop displacements: the displacement of loop residues 47−56, which is necessary for catalysis, followed by displacement and increased disorder of loop residues 25−27 and 33−36. These connected structural changes observed in the Arg7Lys mutant structure suggest a model for toxin activation based on the same structural changes, occurring in a reverse order. Thus a possible scenario for activation of LT and CT, which is schematically represented in Figure 7, is as follows:

Step 1: Reduction and nicking may result in either dissociation of the A_2 fragment from the A_1 subunit or a reorientation of the A_1 and A_2 fragments while the two subunits remain associated. It has been shown that association of the two fragments after activation can occur and that the A_1/A_2 activated complex still contains high levels of ADP-ribosylation activity (Mekalanos et al., 1979a). Hence dissociation of A_1 from A_2 is not a requirement for full activity.

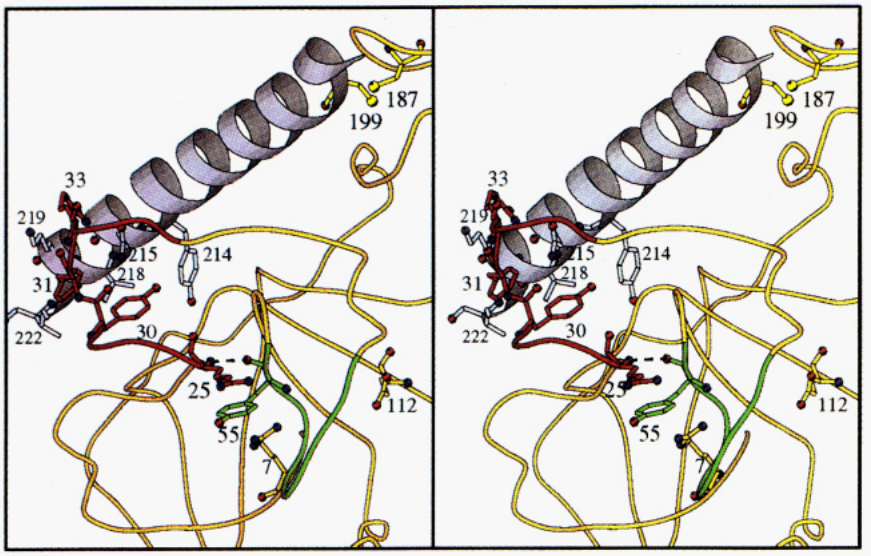

FIGURE 6: Stereo diagram of the A subunit of the wild-type LT. Loop 47−56 is shown in green and loop 25−37 in red. The A_2 helix is shown in purple while the rest of the A subunit is shown in yellow. The following residues are shown in ball-and-stick representation: Arg7, Tyr30, Phe31, Arg33, Tyr55, Glu112, Cys187, Cys199, Tyr214, Asn215, Val218, and Lys219. The hydrogen bond between the backbone carbonyl oxygen of Tyr55 and the backbone nitrogen of Arg25 is highlighted. The distance between these atoms is 2.8 Å.

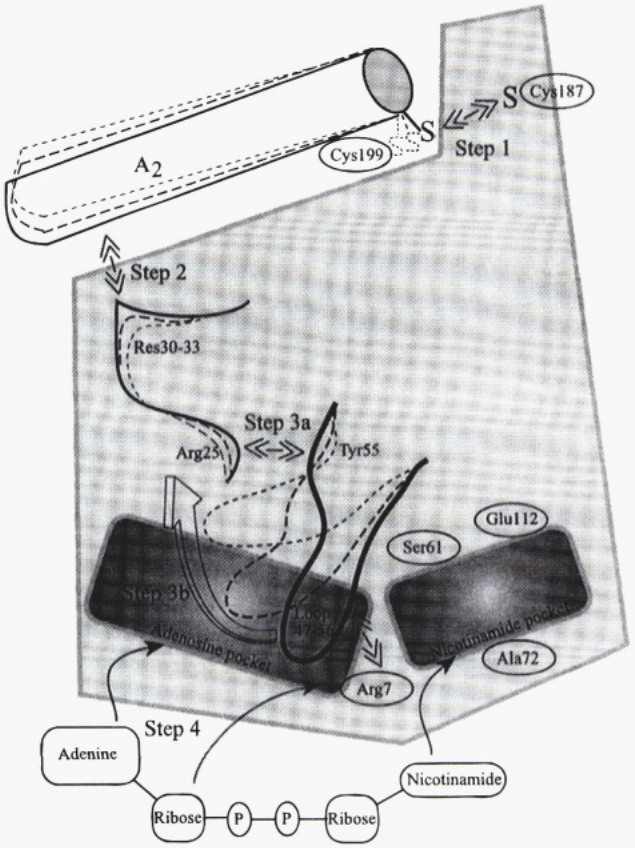

FIGURE 7: Schematic diagram showing the postulated conformational changes in the A subunit upon activation of heat-labile enterotoxin resulting in the displacement of loop 47−56, making the active site accessible for NAD.

Step 2: Residues A:Tyr30, Phe31, and Arg33 of A_1, which are in contact with residues 214, 215, 218, and 219 of the A_2 helix, change position (see Figure 6 and Table 4) as a result of a positional shift of the A_2 helix. Residues 30−33 form the least flexible part of loop 25−36 which has quite high temperature factors for residues 25−27 and 33−36 (Sixma et al., 1993). Residues on either side of 30−33 are also found to be quite mobile in the Arg7Lys mutant structure as can be seen also in Figure 1. Displacement of residues 30−33 may thus cause the entire loop of residues 25−36 to move.

Table 4: Interactions between Residues 30−33 and the A_2-Helix in the Wild-Type LT Structure

atom in loop A:30−33−atom in A_2-helix	distance (Å)
O (Tyr30)−NE2 (Gln215)	2.8
CE2 (Tyr30)−CG (Gln215)	3.8
CZ (Tyr30)−CG (Gln215)	3.9
CD1 (Phe31)−CE (Lys219)	3.8
CE1 (Phe31)−CG (Lys219)	3.8
CE1 (Phe31)−CE (Lys219)	4.0
CE2 (Phe31)−CD1 (Ile222)	3.9
CZ (Phe31)−CG1 (Val218)	3.8
CZ (Phe31)−CG (Lys219)	3.9
NH1(Arg33)−OE1 (Gln215)	3.1
NH2(Arg33)−OE1 (Gln215)	3.4

Table 5: Interactions between Arg25 and Tyr55 in Wild-Type LT

atom of Arg25−atom of Tyr55	distance (Å)
N (Arg25)−O (Tyr55)	2.8
CA (Arg25)−CD2 (Tyr55)	4.0
CA (Arg25)−CE1(Tyr55)	3.7
CA (Arg25)−CZ (Tyr55)	3.9
CB (Arg25)−CE1 (Tyr55)	3.7
CB (Arg25)−CE2 (Tyr55)	3.8
CB (Arg25)−CZ (Tyr55)	3.6

Step 3: Displacement of loop 25−36 disrupts the hydrogen bond between the backbone nitrogen of Arg25 and the backbone carbonyl oxygen of Tyr55. Also the hydrophobic interaction between the hydrophobic parts of the two side chains of these residues might be disrupted (see Table 5 and Figure 6). These disruptions can cause the residues in loop 47−56 to become displaced or susceptible to displacement upon substrate binding. This proposed event would be analogous to the displacement of the same loop upon disruption of the hydrogen bond between the Arg7 side chain and loop 47−56 as observed in the Arg7Lys structure.

Step 4: NAD enters the active site cleft probably causing loop 47−56 to move away, allowing an interaction between Arg7 and the adenosine ribose of NAD. The LTA_1−NAD complex is possibly stabilized by a different conformation of loop A:47−56 as indicated by the stability of the nicked

LTA_I–NAD complex (Galloway & van Heyningen, 1987). This loop might well close the active site again, thereby "embracing" the substrate NAD.

Obviously these hypotheses have to be tested by further mutagenesis and kinetic studies as well as by structural investigations.

CONCLUSION

There is strong evidence that the loop comprising residues 47–56 in LT and CT must move out of the way in order for NAD to bind. The crystal structure of LT containing a substitution of Lys for Arg at residue 7 shows just such a displacement of this loop. The shift in residues 47–56 exposes Arg7 to solvent and thus makes it accessible for an interaction with the ribose of the adenosine moiety of NAD. The Arg7 side chain has thus a double role: when LT is in the latent inactive form, Arg7 holds the 47–56 loop in the conformation previously seen in wild-type LT structures, rendering the active site inaccessible to NAD; when LT is activated and loop 47–56 is displaced, the same residue assists in NAD binding. The dramatic decrease in activity of LT due to the mutation Arg7Lys is thus most likely due to a combination of loss of interaction with NAD and widening of the active site crevice by 1.0 Å.

ACKNOWLEDGMENT

We thank Stewart Turley for assistance with data collection and processing. We also thank Randy Read for the pertussis toxin coordinates.

REFERENCES

Allured, V. S., Collier, R. J., Carroll, S. F., & McKay, D. B. (1986) *Proc. Natl. Acad. Sci. U.S.A. 83*, 1320–1324.

Antoine, R., Tallet, A., van Heyningen, S., & Locht, C. (1993) *J. Biol. Chem. 268*, 24149–24155.

Bennett, M. J., Choe, S., & Eisenberg, D. (1994) *Protein Sci. 3*, 1444–1463.

Black, R. E. (1986) in *Development of vaccines and drugs against diarrhea, 11th Nobel Conference, Stockholm, 1985* (Holmgren, J., Lindberg, A., & Mollby, R., Eds.) pp 23–32, Studentliteratur, Lund, Sweden.

Brandhuber, B. J., Allured, V. S., Falbel, T. G., & McKay, D. B. (1988) *Proteins 3*, 146–154.

Brunger, A. T., Kuriyan, J., & Karplus, M. (1987) *Science 235*, 458–460.

Brunger, A. T., Krukowski, A., & Erickson, J. W. (1990) *Acta Crystallogr. A46*, 585–593.

Burnette, W. N., Mar, V. L., Platler, B. W., Schlotterbeck, J. D., McGinley, M. D., Stoney, K. S., Rohde, M. F., & Kaslow, H. R. (1991) *Infect. Immun. 59*, 4266–4270.

Carrol, S. F., & Collier, R. J. (1984) *Proc. Natl. Acad. Sci. U.S.A. 81*, 3307–3311.

Carrol, S. F., & Collier, R. J. (1987) *J. Biol. Chem. 262*, 8707–8711.

Cassel, D., & Pfeuffer, T. (1978) *Proc. Natl. Acad. Sci. U.S.A. 75*, 2669–2673.

Choe, S., Bennett, M. J., Fujii, G., Curmi, P. M. G., Kantardjieff, K. A., Collier, R. J., & Eisenberg, D. (1992) *Nature 357*, 216–222.

Cieplak, W., Jr., Locht, C., Mar, V. L., Burnette, W. N., & Keith, J. M. (1990) *Biochem. J. 268*, 547–551.

Connelly, M. L. (1983) *J. Appl. Crystallogr. 16*, 548–558.

Domenighini, M., Montecucco, C., Ripka, W. C., & Rappuoli, R. (1991) *Mol. Microbiol. 5*, 23–31.

Douglas, C. M., & Collier, R. J. (1990) *Biochemistry 29*, 5043–5049.

Eidels, L., Proia, R. L., & Hart, D. A. (1983) *Microbiol. Rev. 47*, 596–620.

Galloway, T. S., & van Heyningen, S. (1987) *Biochem. J. 244*, 225–230.

Gill, D. M. (1976) *Biochemistry 15*, 1242–1248.

Harford, S., Dykes, C. W., Hobden, A. N., Read, M. J., & Halliday, I. J. (1989) *Eur. J. Biochem. 183*, 311–316.

Howard, A. J., Gilliland, G. L., Finzel, B. C., Poulous, T. L., Ohlendorf, D. H., & Salemme, F. R. (1987) *J. Appl. Crystallogr. 20*, 383–387.

Johnson, V. G., & Nicholls, P. J. (1994) *J. Biol. Chem. 269*, 4349–4354.

Jones, T. A., Zou, J.-Y., Cowan, S. W., & Kjeldgaard, M. (1991) *Acta Crystallogr. A47*, 110–119.

Kraulis, P. J. (1991) *J. Appl. Crystallogr. 24*, 946–950.

Lobet, Y., Cluff, C. W., & Cieplak, W., Jr. (1991) *Infect. Immun. 59*, 2870–2879.

Mekalanos, J. J., Collier, R. J., & Romig, W. R. (1979a) *J. Biol. Chem. 254*, 5855–5861.

Mekalanos, J. J., Collier, R. J., & Romig, W. R. (1979b) *J. Biol. Chem. 254*, 5849–5854.

Merritt, E. A., Pronk, S. E., Sixma, T. K., Kalk, K. H., van Zanten, B. A. M., & Hol, W. G. J. (1994a) *FEBS Lett. 337*, 88–92.

Merritt, E. A., Sixma, T. K., Kalk, K. H., van Zanten, B. A. M., & Hol, W. G. J. (1994b) *Mol. Microbiol. 13*, 745–753.

Moss, J., Manganiello, V. C., & Vaughan, M. (1976) *Proc. Natl. Acad. Sci. U.S.A. 73*, 4424–4427.

Moss, J., Osborne, J. C., Jr., Fishman, P. H., Nakaya, S., & Robertson, D. C. (1981) *J. Biol. Chem. 256*, 12861–12865.

Papini, E., Schiavo, G., Sandona, D., Rappuoli, R., & Montecucco, C. (1989) *J. Biol. Chem. 264*, 12385–12388.

Papini, E., Schiavo, G., Rappuoli, R., & Montecucco, C. (1990) *Toxicon 28*, 631–635.

Papini, E., Santucci, A., Schiavo, G., Domenighini, M., Neri, P., Rappuoli, R., & Montecucco, C. (1991) *J. Biol. Chem. 266*, 2494–2498.

Pizza, M., Domenighini, M., Hol, W., Giannelli, V., Fontana, M. R., Giuliani, M. M., Magagnoli, C., Peppoloni, S., Manetti, R., & Rappuoli, R. (1994) *Mol. Microbiol. 14*, 51–60.

Pronk, S. E., Hofstra, H., Groendijk, H., Kingma, J., Swarte, M. B. A., Dorner, F., Drenth, J., Hol, W. G. J., & Witholt, B. (1985) *J. Biol. Chem. 260*, 13580–13584.

Ramakrishnan, C., & Ramachandran, G. N. (1965) *Biophys. J. 5*, 909–933.

Read, R. J. (1986) *Acta Crystallogr. A42*, 140–149.

Sixma, T. K., Pronk, S. E., Kalk, K. H., Wartna, E. S., van Zanten, B. A. M., Witholt, B., & Hol, W. G. J. (1991) *Nature 351*, 371–377.

Sixma, T. K., Aguirre, A., Terwisscha van Scheltinga, A. C., Wartna, E. S., Kalk, K. H., & Hol, W. G. J. (1992) *FEBS Lett. 305*, 81–85.

Sixma, T. K., Kalk, K. H., van Zanten, B. A. M., Dauter, Z., Kingma, J., Witholt, B., & Hol, W. G. J. (1993) *J. Mol. Biol. 230*, 890–918.

Stein, P. E., Boodhoo, A., Armstrong, G. D., Cockle, S. A., Klein, M. H., & Read, R. J. (1994) *Structure 2*, 45–57.

Tomasi, M., Battistini, A., Araco, A., Roda, L. G., & D'Agnolo, G. (1979) *Eur. J. Biochem. 93*, 621–627.

Tsuji, T., Inoue, T., Miyama, A., Okamoto, K., Honda, T., & Miwatani, T. (1990) *J. Biol. Chem. 265*, 22520–22525.

Tsuji, T., Inoue, T., Miyama, A., & Noda, M. (1991) *FEBS Lett. 291*, 319–321.

Van Heyningen, S. (1983) *Curr. Top. Membr. Transp. 18*, 445–471.

Wierenga, R. K., Noble, M. E., Postma, J. P., Groendijk, H., Kalk, K. H., Hol, W. G. J., & Opperdoes, F. R. (1991) *Proteins 10*, 33–49.

Wilson, B. A., Reich, K. A., Weinstein, B. R., & Collier, R. J. (1990) *Biochemistry 29*, 8643–8651.

BI950666J